RESEARCH ARTICLE

Active Shimmy Control Method for Driverless Electric Vehicle Considering Unknown Sensor Measurement Error via Sampled-Data Output Feedback

QINGHUA MENG[1], **SHENCHENG ZHAO**[1], **RONG LIU**[1], **ZONG-YAO SUN**[2], **AND HAIBIN HE**[3]

[1]School of Mechanical Engineering, Hangzhou Dianzi University, Hangzhou 310018, China
[2]Institute of Automation, Qufu Normal University, Qufu 273165, China
[3]Ningbo C.S.I. Power & Machinery Group Company Ltd., Ningbo 315000, China

Corresponding author: Qinghua Meng (mengqinghua@hdu.edu.cn)

ABSTRACT Compared with traditional vehicles, driverless electric vehicles equipped with electric wheels are more likely to generate the front wheel shimmy phenomenon, which affects driving comfort and safety. It is necessary to study an active control approach to alleviate or even eliminate the shimmy phenomenon. The current active shimmy control methods do not consider the sensor measurement error. However, the sensor measurement error worsens the effect of an active shimmy control method in practice. For addressing this issue, this paper proposed a novel active shimmy control method considering unknown sensor measurement error via sampled-data output feedback. Firstly, a four-degree-of-freedom (4-DOF) shimmy model of the front electric wheel is built. The dynamic functions of the model are obtained via the Lagrange theorem. Based on the dynamic functions, a shimmy control system with unknown sensor measurement error and nonlinearities is proposed. Then a sampled-data output feedback control (SOFC) method is proposed for the shimmy control system. By selecting an appropriate domination gain, the designed controller can globally asymptotically stabilize the system even in the presence of unknown measurement error. Finally, the 4-DOF shimmy model and the SOFC method for the shimmy system are verified via simulation. The simulation results show that the SOFC method can address the sensor measurement error issue.

INDEX TERMS Vehicle control, driverless electric vehicle, shimmy control, sensor measurement error, sampled-data output feedback.

I. INTRODUCTION

With the development of computer, artificial intelligence, sensor, and internet technologies, the driverless vehicle is greatly developed [1], [2], [3], [4]. Driverless electric vehicle with electric wheel (DEV-EW) especially meets the requirement for energy saving, environmental protection, and handling stability. For a DEV-EW, it is easier to generate a front-wheel shimmy phenomenon than a traditional fuel

The associate editor coordinating the review of this manuscript and approving it for publication was Jjun Cheng.

vehicle because of the electric wheel and no driver interference. The in-wheel motor is fixed into the wheel which changes the mass moment of inertia of the wheel, the tyre cornering stiffness coefficient, the natural frequency, the tyre lateral stiffness coefficient, and the torsional damping of the wheel rotation around kingpin etc. Therefore it is more necessary to study the front electric wheel shimmy model and active control method for the DEV-EW [5], [6], [7].

Many achievements have been obtained on the front wheel shimmy mechanism of traditional fuel vehicles in the past decades. Pacejka analyzed the shimmy phenomenon

considering the tyre characteristics, coulomb friction in the king-pin bearings, and clearance in the wheel bearings [8]. Lu et al. built a 6-DOF dynamic model of a vehicle shimmy system considering the clearance in [9] and stochastic clearance in [10]. Zhuravlev et.al. used poly component dry friction theory to explain the shimmy phenomenon in [11]. Ran et.al. used the Von Schlippe tyre model and the energy flow method to illustrate the energy transfer by the tyre during shimmy in [12]. Bian et al. built a 5-DOF model to analyze the suspension damping characteristics influence on the wheel shimmy of four wheel-independent-drive electric vehicles [13]. Wei et al. analyzed shimmy bifurcation characteristics based on a 4-DOF model in [14] and established a 7-DOF dynamic model of whole vehicle self-excited vibration induced by the shimmy of front wheels which considering the nonlinear factor of tire lateral force and dry friction force in suspension and steering system in [15]. By the way, some researchers also studied the shimmy phenomenon of the aircraft land wheel widely [16], [17].

The aforementioned achievements are about the shimmy mechanism. They are mainly used for vehicle design. Once the shimmy appears, it needs to find effective methods to address this issue. Some researchers have proposed different control methods to alleviate or even eliminate the shimmy phenomenon. For example, Dutta and Choi designed an adaptive sliding mode controller for an automotive steering system with a magneto-rheological damper based on a 4-DOF dynamic model in [18]. Meng et.al. built a 2-DOF shimmy dynamic model of an EV and proposed an active shimmy control method based on sampled-data output feedback in [19]. Then they built a new 4-DOF steering wheel shimmy dynamic model of an EV with independent suspension and constructed an active shimmy controller based on finite-time control method via a nonlinear uncertain disturbance observer to deal with the shimmy phenomenon in [20].

But aforementioned active shimmy control methods do not consider the sensor measurement error. They need precise measurement data acquired by sensors, i.e., there are no sensor measurement errors in the state equations. A universal control system can be described as [21]

$$\dot{x}_i = x_{i+1} + \phi_i(t, x, u), \ i = 1, 2, \cdots, n-1,$$
$$\dot{x}_n = u + \phi_n,$$
$$y = h(t)x_1, \tag{1}$$

where $x = [x_1, \cdots, x_n]^T \in \mathbb{R}^n$, $u \in \mathbb{R}$ and $y \in \mathbb{R}$. The sensor measurement precision $h(t)$ is selected as $h(t) \equiv 1$ directly in most existing control methods. However, there always exists a sensor measurement error because of the sensor design, sensor manufacturing, working temperature, electromagnetic interference, etc, i.e., $h(t) \neq 1$ in engineering and the sensor measurement precision $h(t)$ is bounded unknown or time-variable. In practical shimmy system, sensor measurement errors may manifest in multiple forms. The shimmy system acquires state through the angle sensor installed on the steering column, and then uses the

state observer to obtain the shimmy angle based on the obtained state. The data measured by the sensor contains several errors: a) Random error: Random error is typically caused by factors such as noise, electromagnetic disturbance, and temperature fluctuations in the environment. This error leads to large fluctuations in measurement data, affecting accurate judgments of the measured parameters. b) System error: System error is typically caused by inherent defects in the sensor, calibration errors, or long-term stability issues. System error results in a fixed deviation in all measurements for the sensor. c) Linear error: Linear error causes a fixed proportional deviation between the true value of the measurement and the value of the sensor display. d) Nonlinear error: Nonlinear error causes a complex nonlinear relationship between the true value of the measurement and the value of the sensor display. e) Thermal drift error: Due to the large temperature variations in the automotive operating environment, thermal drift error can cause measurement values to vary at different temperatures. It is challenging for constructing a control law to stabilize the system (1) if the sensor measurement error is considered. But it is necessary to find a new control method to solve this problem via advanced control theory. Some researchers have discussed the control methods considering sensor measurement sensitivity in theory. For example, in [22], Zhang et.al. provided a solution by a feat of the concept of tuning functions and barrier Lyapunov functions. Oh and Choi designed a gain-scaling output feedback controller for a kind of nonlinear system with unknown measurement sensitivity in [23] and studied the regulation of a class of nonlinear systems with unknown growth rate and uncertain measurement sensitivity in [24]. Koo and Choi designed an output feedback controller and discussed the bound of the measurement sensitivity for a class of lower triangular nonlinear systems in [25]. In [26], Liu et.al. presented a new method to obtain the bound of the sensor sensitivity as large as possible. Qian, CJ et al. designed a dynamic output feedback controller to stabilize a nonlinear system with unknown structure and measurement sensitivity [27]. In [28], Deng et.al. studied the event-triggered control of the nonstrict-feedback nonlinear system with unknown measurement and unknown model dynamics. These achievements are focused on continuous time and studied in theory. But in vehicle control systems, the computers are used widely. The computers deal with discrete data, i.e., the outputs of the controllers and inputs of sensors are sampled-data. On the other hand, the nonlinearities and unknown disturbances are generated from the dynamic model of a plant, whose parameters are determined by the parameters of the plant. Therefore, how to design an output feedback controller based on the sampled-data for the front wheel shimmy control system with sensor measurement error is challenging but interesting. In this paper, we will construct a novel sampled-data state observer which can counteract the nonlinearities and unknown sensor measurement error via domination gain, and design a sampled-data output feedback active shimmy controller based on

the constructed observer. The novelties of this paper are as follows.

(1) A 4-DOF electric wheel shimmy model of a DEV-EW is established to express the characteristics of the shimmy phenomenon which also enable the control system to be controllable and observable.

(2) A sampled-data observer with a domination gain is constructed. The domination gain can deal with the nonlinearities and unknown sensor measurement error.

(3) A sample-data output feedback active shimmy controller is designed to stabilize the 4-DOF shimmy system globally asymptotically. The controller can mitigate or even eliminate the negative influence of the unknown sensor measurement error and nonlinearities effectively.

This paper consists of the following sections. The 4-DOF shimmy model of a DEV-EW is established in section II. The sampled-data observer and output feedback controller of the shimmy control system are designed in Section III. Simulations are carried out to verify the effectiveness of the shimmy model and SOFC compared with the SMC method in Section IV. The conclusion of the paper is given in Section V.

II. 4-DOF ELECTRIC WHEEL SHIMMY MODEL OF A DEV-EW

For describing the characteristics of electric wheel shimmy and enabling the controllability of shimmy control system, we simplify the shimmy system to a 4-DOF dynamic model as shown in Figure 1, where θ_1 and θ_2 are the shimmy angles of the front-left wheel and front-right wheel respectively, θ_3 is the swing angle of the pinion, θ_4 is the torsion angle of the motor output shaft, J_1 is the mass moment of inertia of the front-left wheel, J_2 is the mass moment of inertia of the front-right wheel, J_3 is the mass moment of inertia of the pinion, J_4 is the mass moment of inertia of the motor, $\widetilde{k}_1$ is the equivalent torsional stiffness between the front-left wheel and pinon, $\widetilde{k}_2$ is the equivalent torsional stiffness between the front-right wheel and pinion, $\widetilde{k}_3$ is the equivalent torsional stiffness between the pinion and rack, $\widetilde{k}_4$ is the equivalent torsional stiffness between the reduction gear and the motor, k_α is the amplifying coefficient between a steering wheel and the rack of the rack and pinion steering gear, k_β is the amplifying coefficient of the rack and pinion steering gear, c_1 is the torsional damping between the front-left wheel and the rack, c_2 is the torsional damping between the front-right wheel and the rack, c_{l1} is the torsional damping of the front-left wheel rotation around kingpin, c_{r2} is the torsional damping of the front-right wheel rotation around kingpin, c_3 is the torsional damping of the rack, c_g is the equivalent torsional damping between the pinion and rack, c_s is the equivalent torsional damping between the reduction gear and the motor.

According to Lagrange's theorem, there exists

$$\frac{d}{dt}\left(\frac{\partial T}{\partial \dot{q}_i}\right) - \frac{\partial T}{\partial q_i} + \frac{\partial U}{\partial q_i} + \frac{\partial D}{\partial \dot{q}_i} = Q_i \quad (i = 1, 2, 3, 4), \quad (2)$$

where

$$T = \frac{1}{2}J_1\dot{\theta}_1^2 + \frac{1}{2}J_2\dot{\theta}_2^2 + \frac{1}{2}J_3\dot{\theta}_3^2 + \frac{1}{2}J_4\dot{\theta}_4^2,$$

$$U = \frac{1}{2}\widetilde{k}_1(\theta_1 - k_\alpha\theta_3)^2 + \frac{1}{2}\widetilde{k}_2(\theta_2 - k_\alpha\theta_3)^2$$
$$+ \frac{1}{2}\widetilde{k}_3(\theta_3 - k_\beta\theta_4)^2 + \frac{1}{2}\widetilde{k}_4\theta_4^2,$$

$$D = \frac{1}{2}c_{l1}\dot{\theta}_1^2 + \frac{1}{2}c_1(\dot{\theta}_1 - k_\alpha\dot{\theta}_3)^2 + \frac{1}{2}c_{r2}\dot{\theta}_2^2 + \frac{1}{2}c_2(\dot{\theta}_2 - k_\alpha\dot{\theta}_3)^2$$
$$+ \frac{1}{2}c_3(\dot{\theta}_3 - k_\beta\dot{\theta}_4)^2 + \frac{1}{2}c_g\dot{\theta}_3^2 + \frac{1}{2}c_s\dot{\theta}_4^2,$$

q_i is the generalized coordinate which represents $\theta_1, \theta_2, \theta_3, \theta_4$. For a tyre, the motion around a kingpin is mainly caused by lateral force and other external disturbances. Therefore, the generalized force Q_i can be obtained as follows.

$$Q_1 = -F_{yl}(t_m + r_d\sin\alpha) + w_1 - u,$$
$$Q_2 = -F_{yr}(t_m + r_d\sin\alpha) + w_2 - u,$$
$$Q_3 = 0, \quad Q_4 = 0, \quad (3)$$

where F_{yl} and F_{yr} are the lateral forces of the front-left wheel and the front-right wheel respectively, t_m is the pneumatic trail, r_d is the wheel rolling radius, α is the caster angle, w_1 is the moment generated by uncertain disturbances to the front-left wheel and kingpin, w_2 is the moment generated by uncertain disturbances to the front-right wheel and kingpin.
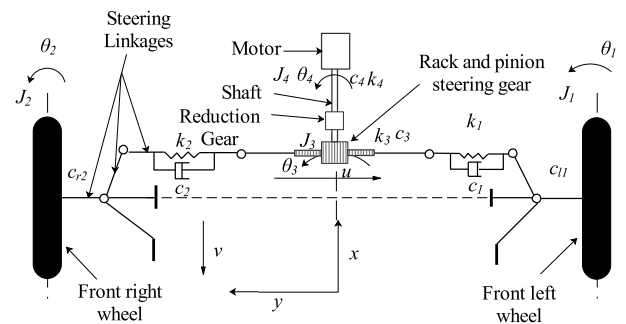

FIGURE 1. The 4-DOF electric wheel shimmy model of a driverless electric vehicle.

For fully reflecting the shimmy characteristics, we use Eq.4 to obtain the lateral forces. The lateral forces are strongly nonlinear.

$$F_{yl} = ak(\theta_1 - b\dot{\theta}_1) + a^2\widetilde{a}_2(\theta_1 - b\dot{\theta}_1)^2 + a^3\widetilde{a}_3(\theta_1 - b\dot{\theta}_1)^3,$$
$$F_{yr} = ak(\theta_2 - b\dot{\theta}_2) + a^2\widetilde{a}_2(\theta_2 - b\dot{\theta}_2)^2 + a^3\widetilde{a}_3(\theta_2 - b\dot{\theta}_2)^3,$$
$$(4)$$

where $a, b, \widetilde{a}_2$, and $\widetilde{a}_3$ are obtained from

$$a = [(\rho v/k)^2 + (\rho f/k)\omega^2]/[\omega^2 + (\rho v/k)^2],$$
$$b = [\rho v/k - \rho^2 fv/k^2]/[(\rho v/k)^2 + \rho f\omega^2/k],$$
$$\widetilde{a}_2 = -0.0668k^2/(\mu G_z), \widetilde{a}_3 = -0.1032k^3/(\mu G_z)^2, \quad (5)$$

where v is the vehicle speed, k is the tyre cornering stiffness coefficient, ω is the natural frequency, ρ is the tyre lateral

stiffness coefficient, G_z is the front wheel vertical weight, μ is the road adhesion coefficient.

Then the 4-DOF dynamic equations are described as

$$J_1\ddot{\theta}_1 + [c_1 + c_{l1} - abk(t_m + r_d\sin\alpha)]\dot{\theta}_1$$
$$+ [\widetilde{k}_1 + ak(t_m + r_d\sin\alpha)]\theta_1 - \widetilde{k}_1 k_\alpha \theta_3$$
$$- c_1 k_\alpha \dot{\theta}_3 + [a^2\widetilde{a}_2(\theta_1 - b\dot{\theta}_1)^2 + a^3\widetilde{a}_3(\theta_1 - b\dot{\theta}_1)^3]$$
$$\cdot (t_m + r_d\sin\alpha) - w_1 + U = 0,$$
$$J_2\ddot{\theta}_2 + [c_2 + c_{r2} - abk(t_m + r_d\sin\alpha)]\dot{\theta}_2$$
$$+ [\widetilde{k}_2 + ak(t_m + r_d\sin\alpha)]\theta_2 - \widetilde{k}_2 k_\alpha \theta_3$$
$$- c_2 k_\alpha \dot{\theta}_3 + [a^2\widetilde{a}_2(\theta_2 - b\dot{\theta}_2)^2 + a^3\widetilde{a}_3(\theta_2 - b\dot{\theta}_2)^3]$$
$$\cdot (t_m + r_d\sin\alpha) - w_2 + U = 0,$$
$$J_3\ddot{\theta}_3 + (c_1 k_\alpha^2 + c_2 k_\alpha^2 + c_3 + c_g)\dot{\theta}_3 - c_1 k_\alpha \dot{\theta}_1$$
$$- c_2 k_\alpha \dot{\theta}_2 - c_3 k_\beta \dot{\theta}_4 - \widetilde{k}_1 k_\alpha \theta_1 - \widetilde{k}_2 k_\alpha \theta_2$$
$$+ (\widetilde{k}_1 k_\alpha^2 + \widetilde{k}_2 k_\alpha^2 + \widetilde{k}_3)\theta_3 - \widetilde{k}_3 k_\beta \theta_4 = 0,$$
$$J_4\ddot{\theta}_4 + (c_3 k_\beta^2 + c_s)\dot{\theta}_4 - \widetilde{k}_3 k_\beta \theta_3 - c_s k_\beta \dot{\theta}_3$$
$$+ (\widetilde{k}_3 k_\beta^2 + \widetilde{k}_4)\theta_4 = 0. \tag{6}$$

Define x_i as

$$x_1(t) = \theta_4(t), \quad x_2(t) = \dot{\theta}_4(t), \quad x_3(t) = \frac{\widetilde{k}_3 k_\beta}{J_4}\theta_3(t)$$

$$x_4(t) = \frac{\widetilde{k}_3 k_\beta}{J_4}\dot{\theta}_3(t), \quad x_5(t) = \frac{\widetilde{k}_2\widetilde{k}_3 k_\alpha k_\beta}{J_3 J_4}\theta_2(t)$$

$$x_6(t) = \frac{\widetilde{k}_2\widetilde{k}_3 k_\alpha k_\beta}{J_3 J_4}\dot{\theta}_2(t), \quad x_7(t) = \frac{\widetilde{k}_1\widetilde{k}_3 k_\alpha k_\beta}{J_3 J_4}\theta_1(t)$$

$$x_8(t) = \frac{\widetilde{k}_1\widetilde{k}_3 k_\alpha k_\beta}{J_3 J_4}\dot{\theta}_1(t). \tag{7}$$

The state equations of Eq.6 are

$$\dot{x}_i(t) = x_{i+1}(t) + \phi_i(t, x(t)), \quad i = 1, 2, \cdots, 7$$
$$\dot{x}_8(t) = u(t) + \phi_8(t, x(t))$$
$$y = h(t)x_1(t), \tag{8}$$

where

$$\phi_1(t, x(t)) = 0,$$
$$\phi_2(t, x(t)) = -\frac{\widetilde{k}_3 k_\beta^2 + \widetilde{k}_4}{J_4}x_1 - \frac{c_3 k_\beta^2 + c_3}{J_4}x_2 + \frac{c_s}{\widetilde{k}_3}x_4,$$
$$\phi_3(t, x(t)) = 0,$$
$$\phi_4(t, x(t)) = \frac{\widetilde{k}_3^2 k_\beta^2}{J_3 J_4}x_1 + \frac{c_3\widetilde{k}_3 k_\beta^2}{J_3 J_4}x_2 - \frac{\widetilde{k}_1 k_\alpha^2 + \widetilde{k}_2 k_\alpha^2 + \widetilde{k}_3}{J_3}x_3$$
$$- \frac{c_1 k_\alpha^2 + c_2 k_\alpha^2 + c_3 + c_g}{J_3}x_4 + \frac{c_2}{\widetilde{k}_2}x_6 + x_7 + \frac{c_1}{\widetilde{k}_1}x_8,$$

$$\phi_5(t, x(t)) = 0,$$
$$\phi_6(t, x(t)) = \frac{\widetilde{k}_2^2 k_\alpha^2}{J_2 J_3}x_3 + \frac{c_2 k_\alpha^2 k_2}{J_2 J_3}x_4$$
$$- \frac{\widetilde{k}_2 + ak(t_m + r_d\sin\alpha)}{J_2}x_5$$
$$- \frac{c_2 + c_{r2} - abk(t_m + r_d\sin\alpha)}{J_2}x_6$$

$$- x_7 + L_1 + \frac{\widetilde{k}_2\widetilde{k}_3 k_\alpha k_\beta}{J_2 J_3 J_4}w_2 - \frac{\widetilde{k}_2\widetilde{k}_3 k_\alpha k_\beta}{J_2 J_3 J_4}U,$$
$$\phi_7(t, x(t)) = 0,$$
$$\phi_8(t, x(t)) = \frac{\widetilde{k}_1^2 k_\alpha^2}{J_1 J_3}x_3 + \frac{c_1 k_\alpha^2 k_1}{J_1 J_3}x_4$$
$$- \frac{\widetilde{k}_1 + ak(t_m + r_d\sin\alpha)}{J_1}x_7$$
$$- \frac{c_1 + c_{l1} - abk(t_m + r_d\sin\alpha)}{J_1}x_8$$
$$+ L_2 + \frac{\widetilde{k}_1\widetilde{k}_3 k_\alpha k_\beta}{J_1 J_3 J_4}w_1,$$
$$u(t) = -\frac{\widetilde{k}_1\widetilde{k}_3 k_\alpha k_\beta}{J_1 J_3 J_4}U,$$
$$L_1 = -\frac{1}{J_2}\left[a^2\widetilde{a}_2\frac{J_3 J_4}{\widetilde{k}_2\widetilde{k}_3 k_\alpha k_\beta}(x_5 - bx_6)^2 + a^3\widetilde{a}_3\left(\frac{J_3 J_4}{\widetilde{k}_2\widetilde{k}_3 k_\alpha k_\beta}\right)^2(x_5 - bx_6)^3\right]$$
$$\times (t_m + r_d\sin\alpha),$$
$$L_2 = -\frac{1}{J_1}\left[a^2\widetilde{a}_2\frac{J_3 J_4}{\widetilde{k}_1\widetilde{k}_3 k_\alpha k_\beta}(x_7 - bx_8)^2 + a^3\widetilde{a}_3\left(\frac{J_3 J_4}{\widetilde{k}_1\widetilde{k}_3 k_\alpha k_\beta}\right)^2(x_7 - bx_8)^3\right]$$
$$\times (t_m + r_d\sin\alpha).$$

One can find that the state equations include the sensor measurement precision $h(t)$ which means that the torsion angle of the motor output shaft obtained by the torsion angle sensor includes the sensor measurement error caused by external disturbances.

Remark 1: The 4-DOF shimmy model is more precise than some shimmy models. It can meet the requirement of engineering. The higher DOF shimmy models are more precise than the 4-DOF shimmy model. But these models increase the control difficulty greatly. And the real-time performance of higher DOF shimmy models get worse. Taking these factors into consideration, we choose to build this 4-DOF model. We simulate this model in IV section. The simulation results coincide with published achievements which verify that this 4-DOF model is effective.

III. ACTIVE SHIMMY CONTROL APPROACH BASED ON SAMPLED-DATA OUTPUT FEEDBACK

In this section, we will design a linear observer with a domination gain as well as a controller based on sampled-data output feedback for system (8) which considers the unknown sensor measurement precision $h(t)$. To begin with, we provide two assumptions on the nonlinear terms and the unknown sensor measurement error of the system (8) respectively.

Assumption 1: There exists a constant $c \geq 0$ such that

$$|\phi_i(t, x(t), u(t))| \leq c(|x_1| + |x_2| + \cdots + |x_i(t)|), \tag{9}$$
$$i = 1, 2, \cdots, 8$$

for all $(t, x, u) \in \mathbb{R} \times \mathbb{R}^+ \times \mathbb{R}^8$.

Assumption 2: There exists a positive constant $h(t) \in (0, 1)$ such that

$$1 - h^*(t) \le h(t) \le 1 + h^*(t), \qquad (10)$$

for all $t \in \mathbb{R}^+$, where $h^*(t)$ is the allowable sensor measurement error.

Next, we will provide a theorem to express our achievement of this paper.

Theorem 1: A sampled-data output feedback controller designed as

$$u(t) = u(t_k) = -k_1 y(t_k) - k_2 \hat{z}_2(t_k) - \cdots - k_8 \hat{z}_8(t_k),$$
$$\forall t \in [t_k, t_{k+1}), t_k = kT, k = 0, 1, 2, \cdots \quad (11)$$

with an observer

$$\begin{cases} \hat{z}_1(t_k) = z_1(t_k), \hat{z}_i(t) = \hat{\eta}_i(t) + a_i \hat{z}_{i-1}(t), y(t_k) = z_1(t_k), \\ \dot{\hat{\eta}}_i(t) = -La_i \eta_i(t) - La_i^2 \hat{z}_{i-1}(t_k), i = 2, 3, \cdots, 8 \end{cases}$$
$$(12)$$

can globally asymptotically stabilize system (8) with an allowable sensor measurement precision $h(t_k) \in [1 - h^*(t_k), 1 + h^*(t_k)]$ under Assumption 1 and 2 where a_i are coefficients of a Hurwitz polynomial. k_i in Eq.11 are coefficients of a Hurwitz polynomial. $L \ge 1$ is a domination gain to dominate the unknown nonlinear items and unknown sensor measurement error which will be determined in the following section.

Next, we will prove Theorem 1 by the Lyapunov method. Firstly, we give a lemma which helps to prove Theorem 1.

Lemma 1 [29]: The following inequality holds for any $x \in \mathbb{R}$ and $y \in \mathbb{R}$, if select a and b to be positive real numbers.

$$a|x||y| \le b|x|^2 + \frac{a^2}{4b}|y|^2. \qquad (13)$$

Proof: The following work is to prove Theorem 1. We divide the proof process into four parts. Firstly, system (8) is pretreated via coordinate transformation for introducing a domination gain L which is used to dominate the unknown sensor measurement error and nonlinearities. Then a linear sampled-data state observer including the same domination gain L is designed. Next, a sampled-data output feedback control law is proposed based on the domination gain observer. Finally, the allowable sensor measurement error is explicitly determined whereby the domination gain L and sampling period T are appropriately selected to render system (8) globally asymptotically stable.

A. PRETREATMENT OF SYSTEM (8) VIA COORDINATE TRANSFORMATION

We introduce the following coordinate transformation

$$z_1 = x_1, z_i = \frac{x_i}{L^{i-1}}, \quad v = \frac{u}{L^8}, i = 2, 3, \cdots, 7, \qquad (14)$$

It will be determined later. Under the new coordinate $z = [z_1 \, z_2 \, \cdots \, z_8]^T \in \mathbb{R}^8$, system (8) can be written as

$$\dot{z}_1(t) = Lz_2(t) + \bar{\phi}_1(z(t), v(t), t)$$
$$\dot{z}_2(t) = Lz_3(t) + \bar{\phi}_2(z(t), v(t), t)$$

$$\cdots$$
$$\dot{z}_7(t) = Lz_8(t) + \bar{\phi}_7(z(t), v(t), t)$$
$$\dot{z}_8(t) = Lv(t) + \bar{\phi}_8(z(t), v(t), t)$$
$$y(t) = h(t)z_1(t), \qquad (15)$$

where

$$\bar{\phi}_1(z(t), v(t), t) = \phi_1(x(t), u(t), t),$$
$$\bar{\phi}_i(z(t), v(t), t) = \frac{\phi_i(x(t), u(t), t)}{L^{i-1}}, i = 2, 3, \cdots, 8.$$

For an electric wheel shimmy system, the states are limited. Therefore, the nonlinear terms of system (15) meet Assumption 1, i.e.,

$$|\bar{\phi}_i(z(t), v(t), t)| \le \frac{c}{L^{i-1}}(|z_1(t)| + \cdots + |L^{i-1}z_i(t)|). \quad (16)$$

B. DESIGN OF LINEAR SAMPLED-DATA OBSERVER WITH DOMINATION GAIN

According to the observer designed in [30], we construct a sampled-data observer which includes the continuous-time states $\eta_i(t)$ and the discrete $y(t_k)$ as its input signals.

$$\dot{\hat{\eta}}_2(t) = -La_2 \hat{\eta}_2(t) - La_2^2 y(t_k), \hat{z}_2(t) = \hat{\eta}_2(t) + a_2 y(t),$$
$$\dot{\hat{\eta}}_i(t) = -La_i \hat{\eta}_i(t) - La_i^2 \hat{z}_{i-1}(t_k), \hat{z}_i(t) = \hat{\eta}_i(t) + a_i \hat{z}_{i-1}(t),$$
$$(17)$$

for $t \in [t_k, t_{k+1}], i = 3, 4, \cdots, 8$, where a_i are coefficients of a Hurwitz polynomial.

In the observer (17), $\hat{\eta}$ is used to estimate the unmeasurable variable

$$\eta_i(t) = z_i(t) - a_i z_{i-1}(t). \qquad (18)$$

We define

$$\hat{\eta}(t) = [\hat{\eta}_2 \, \hat{\eta}_3(t) \, \cdots \, \hat{\eta}_8(t)]^T, \hat{Z}(t) = [y(t) \, \hat{z}_2(t) \, \cdots \, \hat{z}_7(t)]^T,$$
$$\hat{z}(t) = [\hat{z}_2(t) \, \hat{z}_3(t) \, \cdots \hat{z}_8(t)]^T, A = \text{diag}(a_2, a_3, \cdots, a_8).$$

The observer (17) is rewritten as

$$\dot{\hat{\eta}}(t) = -LA\hat{\eta}(t) - LA^2 \hat{Z}(t_k), \hat{z}(t) = \hat{\eta}(t) + A\hat{Z}(t) \quad (19)$$

for $t \in [t_k, t_{k+1}]$, from which we obtain the estimation

$$\hat{\eta}(t_{k+1}) = e^{LTa}\hat{\eta}(t_k) + L\left(\int_0^T e^{-LTas}ds\right) A^2 \hat{Z}(t_k), \quad (20)$$

and

$$\hat{z}_2(t_k) = \hat{\eta}(t_k) + a_2 y(t_k), \hat{z}_i(t_k) = \hat{\eta}_i(t_k) + a_i \hat{z}_7(t_k),$$
$$i = 3, 4, \cdots, 8. \quad (21)$$

Then the estimation error of $\eta_i, i = 2, 3, \cdots, 8$ is

$$e_i(t) = \eta_i(t) - \hat{\eta}(t), \qquad (22)$$

i.e.,

$$\dot{e}_2(t) = Lz_3(t) - La_2 e_2(t) - La_2^2(z_1(t) - y(t))$$
$$- La_2^2(y(t) - y(t_k)) + \bar{\phi}_2(\cdot) - a_2\bar{\phi}_1(\cdot)$$
$$\dot{e}_3(t) = Lz_4(t) - La_3 e_3(t) - La_3^2(z_2(t) - \hat{z}_2(t))$$

$$- La_3^2(\hat{z}_2(t) - \hat{z}_2(t_k)) + \bar{\phi}_3(\cdot) - a_3\bar{\phi}_2(\cdot)$$

$$\vdots$$

$$\dot{e}_7(t) = Lz_8(t) - La_7e_7(t) - La_7^2(z_6(t) - \hat{z}_6(t))$$
$$- La_7^2(\hat{z}_6(t) - \hat{z}_6(t_k)) + \bar{\phi}_7(\cdot) - a_7\bar{\phi}_6(\cdot)$$

$$\dot{e}_8(t) = Lv(t) - La_8e_8(t) - La_8^2(z_7(t) - \hat{z}_7(t))$$
$$- La_8^2(\hat{z}_7(t) - \hat{z}_7(t_k)) + \bar{\phi}_8(\cdot) - a_8\bar{\phi}_7(\cdot). \quad (23)$$

We define the function V_0 as

$$V_0(e(t)) = \frac{1}{2}e(t)e^T(t), \quad (24)$$

where $e(t) = [e_2(t) \ e_3(t) \ \cdots \ e_8(t))]$.

Via Lemma 1, the time derivative of $V_0(E(t))$ along (23) satisfies

$$\dot{V}_o(e(t))$$
$$\leq -L \sum_{i=2}^{8} a_i e_i^2(t) + L \sum_{i=2}^{7} 2e_i^2(t) + \frac{L}{4}(|z_8(t) + \bar{B}^T Z_8(t)|)^2$$
$$+ L\left(\frac{1}{4}\|\bar{B}\|^2\right)\|Z_7(t)\|^2 + La_2^2|e_2(t)||z_1(t) - y(t)|$$
$$+ L\sum_{i=3}^{8} a_i^2|e_i(t)||z_{i-1}(t) - \hat{z}_{i-1}(t)| + La_2^2|e_2(t)||y(t) - y(t_k)|$$
$$+ L\sum_{i=3}^{8} a_i^2|e_i(t)||\hat{z}_{i-1}(t) - \hat{z}_{i-1}(t_k)| + L|e_8(t)v(t)|$$
$$+ |e_2(t)(\bar{\phi}_2(\cdot) - a_2\bar{\phi}_1(\cdot)) + \cdots + e_8(t)(\bar{\phi}_8(\cdot) - a_8\bar{\phi}_7(\cdot))|, \quad (25)$$

where $t \in [t_k, t_{k+1})$, $\bar{B} = [b_1 \ b_2 \ \cdots \ b_7]^T$ is a set of coefficients of a Hurwitz polynomial.

C. CONSTRUCTION OF THE ACTIVE SHIMMY CONTROL LAW BASED ON SAMPLED-DATA OUTPUT FEEDBACK

For solving the problem of shimmy control system considering unknown sensor measurement error, we design the following sampled-data output feedback controller

$$v(t) = v(t_k) = -k_1 y(t_k) - k_2\hat{z}_2(t_k) - \cdots - k_8\hat{z}_8(t_k),$$
$$\forall t \in [t_k, t_{k+1}), t_k = kT, k = 0, 1, 2, \cdots. \quad (26)$$

Then (15) can be rewritten as

$$\dot{Z}_7(t) = LBZ_7(T) + LC(z_8(t) + \bar{B}^T Z_7(t)) + \bar{\Phi}(\cdot)$$
$$\dot{z}_8(t) = -L(k_1 y(t_k) + k_2\hat{z}(t_k) + \cdots + k_8\hat{z}_8(t_k)) + \bar{\phi}_8(\cdot)$$
$$y(t) = h(t)z_1(t), \quad (27)$$

where

$$Z_7 = [z_1(t) \ z_2(t) \ \cdots \ z_7(t)]^T, C = [0 \ 0 \ \cdots \ 1]^T \in \mathbb{R}^7,$$
$$\bar{\Phi}(\cdot) = [\bar{\phi}_1(\cdot) \ \bar{\phi}_2(\cdot) \ \cdots \ \bar{\phi}_7(\cdot)]^T$$

$$B = \begin{bmatrix} 0 & 1 & \cdots 0 \\ \vdots & \vdots & \ddots & \vdots \\ 0 & 0 & \cdots 1 \\ -b_1 & -b_2 & \cdots & -b_7 \end{bmatrix}.$$

Furtherly, we select the function V_1 as

$$V_1(z(t)) = Z_7^T(t)PZ_7(t) + \frac{(z_8(t) + \bar{B}^T Z_7(t))^2}{2}, \quad (28)$$

where $P \in \mathbb{R}^{7 \times 7}$ is a positive definite matrix which satisfies

$$PB + B^T P = -\left(q + \frac{1}{2}\right)I_7. \quad (29)$$

It is obvious that $V_1(z(t))$ is positive definite. Similar with the processing of $V_0(z(t))$, the time derivative of $V_1(z(t))$ along (27) satisfies

$$\dot{V}_1(z(t)) \leq -Lq\|Z_7(t)\|^2 + L\left(b_7 + \frac{(2\|PC\| + \|\bar{B}^T B\|)^2}{2}\right)$$
$$\cdot (z_8(t) + \bar{B}^T Z_7(t))^2 - L(k_1 z_1(t) + k_2 z_2(t)$$
$$+ \cdots + k_8 z_8(t))(z_8(t) + \bar{B}^T Z_7(t))$$
$$+ 2|Z_7^T(t)P\bar{\Phi}(\cdot)| + L|z_8(t) + \bar{B}^T Z_7(t)|$$
$$\cdot |k_1(z_1(t) - y(t_k)) + k_2(z_2(t) - \hat{z}_2(t))$$
$$+ \cdots + k_8(z_8(t) - \hat{z}_8(t_k))|$$
$$+ |z_8(t) + \bar{B}^T Z_7(t)||\bar{\phi}_8(\cdot) + \bar{B}^T \bar{\Phi}(\cdot)|. \quad (30)$$

We let $k_8 \geq b_7 + \frac{(2\|PC\| + \|\bar{B}^T B\|)^2}{2} + 1$ and $k_i = b_i k_8$, $i = 1, \cdots 7$, then one obtains

$$\dot{V}_1(z(t)) \leq -Lq\|Z_7(t)\|^2 - L(z_8(t) + \bar{B}^T Z_7(t))^2$$
$$+ 2|Z_7^T P\bar{\Phi}(\cdot)| + L|z_8(t) + \bar{B}^T Z_7(t)|$$
$$\cdot |k_1(z_1(t) - y(t_k)) + k_2(z_2(t) - \hat{z}_2(t))$$
$$+ \cdots + k_8(z_8(t) - \hat{z}_8(t_k))|$$
$$+ |z_8(t) + \bar{B}^T Z_7(t)||\bar{\phi}_8(\cdot) + \bar{B}^T \bar{\Phi}(\cdot)|. \quad (31)$$

Then the function $V(z(t), e(t))$ is defines as

$$V(\mathcal{Z}(t)) = V_0(e(t)) + V_1(z(t)) \quad (32)$$

with $\mathcal{Z} = (z(t), e(t))^T \in \mathbb{R}^{15}$.

Before we continue to carry out the proof, we introduce two propositions which are proved in reference [30].

Proposition 1: Letting $a_{i \to i+1} = 1$, $a_{i \to i} = a_i$, $a_{i \to j} = a_i a_{i-1} \cdots j$, for $i = 2, \cdots 8, j = 2, \cdots i - 1$, the following inequality holds,

$$a_2^2|e_2(t)||z_1(t) - y(t)| + \sum_{i=3}^{8} a_i^2|e_i(t)||z_{i-1}(t)|$$
$$\leq \sum_{i=2}^{8}\left(i - 1 + \sum_{j=i+1}^{8} \frac{a_j^2 a_{j \to i+1}^2}{4}\right)e_i^2(t)$$
$$+ \sum_{i=2}^{8} \frac{a_i^2 a_{i \to 2}^2}{4}|z_1(t) - y(t)|^2. \quad (33)$$

Proposition 2: There are nonnegative constants α_1, α_2, α_3, α_4, α_5, α_6, α_7, α_8, and $V_{max}(\mathcal{Z}(t)) = \max V(\mathcal{Z}(s))$,

$s \in [t_k, t)$ such that the following inequalities hold,

$$
\begin{aligned}
2|Z_7^T(t)P\bar{\Phi}(\cdot)| &+ |e_2(t)(\bar{\phi}_2(\cdot) - a_2\bar{\phi}_1(\cdot)) \\
&+ \cdots + e_8(t)(\bar{\phi}_8(\cdot) - a_8\bar{\phi}_7(\cdot))| \\
&+ |z_8(t) + \bar{B}^T Z_7(t)||\bar{\phi}_8(\cdot) + \bar{B}^T\bar{\Phi}(\cdot)| \leq \alpha_1\|\mathcal{Z}(t)\|^2.
\end{aligned}
\tag{34}
$$

$$
\begin{aligned}
L\sum_{i=3}^{8} a_i^2|e_i(t)||\hat{z}_{i-1}(t_k)| &+ La_2^2|e_2(t)||y(t) - y(t_k)| \\
\leq L^2\alpha_2 &\sqrt{V(\mathcal{Z}(t))}\sqrt{V_{\max}(\mathcal{Z}(t))}(t - t_k) \\
&+ L\alpha_3 V(\mathcal{Z}(t)) + L^2\alpha_4\sqrt{V(\mathcal{Z}(t))}|z_1(t) - y(t_k)|(t - t_k).
\end{aligned}
\tag{35}
$$

$$
\begin{aligned}
|z_8(t) + \bar{B}^T Z_7(t)||k_1(z_1(t) &- y(t_k)) + k_2(z_2(t) - \hat{z}_2(t_k)) \\
&+ \cdots + k_8(z_8(t) - \hat{z}_8(t_k))| \\
&+ |e_8(t)(k_1 y(t_k) + \cdots + k_8\hat{z}_8(t_k))| \\
\leq \frac{1}{2}|z_8(t) + \bar{B}^T Z_7(t)|^2 &+ \frac{1}{8}\|Z_7(t)\|^2 + \frac{33}{4}\alpha_5|z_1(t) - y(t)|^2 \\
+ \alpha_6 V(\mathcal{Z}(t)) &+ \frac{33}{4}\sum_{i=2}^{7}\left(\sum_{j=i}^{8} k_j a_{j\to i+1}\right)^2 e_i^2(t) \\
+ L\alpha_7\sqrt{V(\mathcal{V}(t))} &|z_1(t_k) - y(t_k)|(t - t_k) \\
+ \left(\sum_{i=1}^{7} 2(k_i + k_8\|\bar{B}\|)^2 \right. &\left. + 9k_8^2 + k_8 + 7\right) e_8^2(t) \\
+ L\alpha_8\sqrt{V\mathcal{Z}(t)} &\sqrt{V_{\max}(\mathcal{Z}(t))}(t - t_k).
\end{aligned}
\tag{36}
$$

With the help of Propositions 1 and 2, Eq.32 satisfies

$$
\begin{aligned}
\dot{V}(\mathcal{Z}(t)) \leq &- L\left(q - \frac{1}{4}\|\bar{B}\|^2 - \frac{1}{4}\right)\|Z_7(t)\|^2 \\
&- \frac{L}{4}(z_8(t) + \bar{B}^T Z_7(t))^2 - L\sum_{i=2}^{8}(a_i - \delta_i)e_i^2(t) \\
&+ L\delta_1|z_1(t) - y(t)|^2 + \alpha_1\|\mathcal{Z}(t)\|^2 \\
&+ L^2(\alpha_4 + \alpha_7)\sqrt{V\mathcal{Z}(t)}|z_1(t_k) - y(t_k)|(t - t_k) \\
&\times L^2(\alpha_2 + \alpha_8)\sqrt{V\mathcal{Z}(t)}\sqrt{V_{\max}(\mathcal{Z}(t))}(t - t_k) \\
&+ L(\alpha_3 + \alpha_6)V(\mathcal{Z}(t)), t \in [t_k, t_{k+1}),
\end{aligned}
\tag{37}
$$

where

$$
\delta_1 = \sum_{i=2}^{8} \frac{a_i^2 a_{i\to 2}^2}{4} + \frac{33}{4}\alpha_5,
$$

$$
\delta_i = i + 1 + \sum_{j=i+1}^{8} \frac{a_j^2 a_{j\to i+1}^2}{4} + \frac{33}{4}\left(\sum_{j=i}^{8} k_j a_{j\to i+1}\right)^2,
$$

$$
\delta_8 = \sum_{i=1}^{7} 2(k_i + k_8\|\bar{B}\|)^2 + 9k_8^2 + k_8 + 14.
$$

For insuring $\dot{V}(\mathcal{Z}(t))$ to be negative definite, next we will deal with the left items of Eq.37. First, we select $q \geq \frac{1}{4}\|\bar{B}\|^2 + \frac{1}{2}$. Then when $k_i, i = 1, 2, \cdots, 8$ is determined,

$\delta_i, i = 1, 2, \cdots, 8$ depends only on $a_i, i = 2, 3, \cdots, 8$ which can be selected as

$$
a_8 \geq \delta_8 + \frac{1}{4}, \quad a_i \geq \delta_i(a_{i+1}, a_{i+2}, \cdots, a_8) + \frac{1}{4}.
\tag{38}
$$

Because $V(\mathcal{Z}(t))$ is positive definite, there are positive constants $\sigma_i, i = 1, 2, \cdots, 6$ such that

$$
4\sigma_1 V(\mathcal{Z}(t)) \leq \|Z_7(t)\|^2 + |z_8(t) + \bar{B}^T Z_7(t)|^2 + \|e(t)\|^2,
$$
$$
\sigma_2\|\mathcal{Z}(t)\|^2 \leq \sigma_3 V(\mathcal{Z}(t)).
\tag{39}
$$

Via Eq.39, one has

$$
\begin{aligned}
-\left(q - \frac{1}{4}\|\bar{B}\|^2 - \frac{1}{4}\right)\|Z_7(t)\|^2 &- \frac{1}{4}(z_8(t) + \bar{B}^T Z_7(t))^2 \\
- \sum_{i=2}^{8}(a_i - \delta_i)e_i^2(t) & \\
\leq -\frac{1}{4}\|Z_7(t)\|^2 - \frac{1}{4}(z_8(t) &+ \bar{B}^T Z_7(t))^2 - \frac{1}{4}\sum_{i=2}^{8} e_i^2(t) \\
\leq -\sigma_1 V(\mathcal{Z}(t)) &
\end{aligned}
\tag{40}
$$

and

$$
|z_1(t)|^2 \leq \|\mathcal{Z}(t)\|^2 \leq \frac{\sigma_3}{\sigma_2}V(\mathcal{Z}(t)) =: \sigma_4 V(\mathcal{Z}(t)).
\tag{41}
$$

According to Assumption 2, one can obtain

$$
|z_1(t) - y(t)| \leq h(t)\sqrt{\sigma_4}\sqrt{V(\mathcal{Z}(t))},
\tag{42}
$$

therefore

$$
|z_1(t_k) - y(t_k)| \leq h(t)\sqrt{\sigma_4}\sqrt{V(\mathcal{Z}(t_k))}.
\tag{43}
$$

We select the allowable sensor measurement error as

$$
h^* = min\left\{\sqrt{\frac{\sigma_1}{4\delta_1\sigma_4}}, \frac{\sigma_1\sqrt{\lambda_{\min}(P)}}{8\zeta}, 1\right\},
\tag{44}
$$

where

$$
\zeta = 2\sqrt{2}\left(k_1 + \sum_{i=2}^{8} k_i a_{i\to 2}\right) + \sqrt{2}\left(a_2^2 + \sum_{i=3}^{8} a_i a_{i\to 2}\right).
$$

Via (42)-(44), we have

$$
\begin{aligned}
\delta_1|z_1(t) - y(t)|^2 &+ (\alpha_3 + \alpha_6)V(\mathcal{Z}(t)) \\
\leq \delta_1 h^2\sigma_4 V(\mathcal{Z}(t)) &+ \frac{2\zeta h}{\sqrt{\lambda_{\min}(P)}}V(\mathcal{Z}(t)) \\
\leq \frac{\sigma_1}{2}V(\mathcal{Z}(t)) &
\end{aligned}
\tag{45}
$$

and

$$
\begin{aligned}
(\alpha_4 + \alpha_7)\sqrt{V(\mathcal{Z}(t))}&|z_1(t_k) - y(t_k)|(t - t_k) \\
+ (\alpha_2 + \alpha_8)\sqrt{V(\mathcal{Z}(t))V_{\max}(\mathcal{Z}(t))}(t - t_k) & \\
\leq h(\alpha_4 + \alpha_7)\sqrt{V(\mathcal{Z}(t))}&\sqrt{\sigma_4}\sqrt{V(\mathcal{Z}(t_k))}(t - t_k) \\
+ (\alpha_2 + \alpha_8)\sqrt{V(\mathcal{Z}(t))V_{\max}(\mathcal{Z}(t))}(t - t_k) & \\
\leq \sigma_5\sqrt{V(\mathcal{Z}(t))}&\sqrt{V_{\max}(\mathcal{Z}(t))}(t - t_k),
\end{aligned}
\tag{46}
$$

where $\sigma_5 = h^*(\alpha_4 + \alpha_7)\sqrt{\sigma_4} + \alpha_2 + \alpha_8$. Substituting (40),(41), (42), (43), (45), and (46) into (37), one has

$$\dot{V}(\mathcal{Z}(t)) \leq -\frac{L\sigma_1 - 2\alpha_1\sigma_4}{2}V(\mathcal{Z}(t))$$
$$+ L^2\sigma_5\sqrt{V(\mathcal{Z}(t))}\sqrt{V_{\max}(\mathcal{Z}(t))}(t - t_k),$$
$$t \in [t_k, t_{k+1}). \qquad (47)$$

According to the continuity of $V(\mathcal{Z}(t))$, there exists

$$\max V(Z(s))|s \in [t_k, t_{k+1}] = V(Z(t_k)). \qquad (48)$$

According to Eq.47, we select

$$L \geq \frac{2(\sigma_6 + \alpha_1\sigma_4)}{\sigma_1}, T < \frac{\sigma_6}{L^2\sigma_5}, \qquad (49)$$

where $\sigma_6 > 0$ is a constant. Therefore

$$\dot{V}(\mathcal{Z}(t)) \leq -\sigma_6 V(\mathcal{Z}(t))$$
$$+ L^2\sigma_5\sqrt{V(\mathcal{Z}(t))}\sqrt{V(\mathcal{Z}(t_k))}(t - t_k), t \in [t_k, t_{k+1}). \qquad (50)$$

From Eq.50, one can conclude that system (8) can be globally stabilized by the sampled-data observer (17) and controller (11) if T and L are correctly selected according to Eq.49.

Proof ends.

IV. NUMERICAL SIMULATION ANALYSIS

In this section, the established 4-DOF shimmy model of the DEV-EW will be analyzed via numerical simulation. Then the proposed SOFC method for the shimmy system is simulated and compared with the SMC method to verify its effectiveness.

A. THE SHIMMY MODEL SIMULATION

We firstly simulate the 4-DOF shimmy model. The used parameters of the shimmy system are listed in Tab.1.

TABLE 1. The parameters of the designed controller.

Parameter	Nominal Value	Parameter	Nominal Value
$J_{1,2}$	20kg· m^2	J_3	11kg· m^2
J_4	17kg· m^2	$\widetilde{k}_{1,2}$	38000N· m/rad
$\widetilde{k}_3$	60000N· m/rad	$\widetilde{k}_4$	70000N· m/rad
$\widetilde{k}_5$	120000N· m/rad	r	0.012rad
L	0.15m	$c_{1,2}$	20N· m · s/rad
$c_{l1,r2}$	50N· m · s/rad	$c_3{'}$	10N· m · s/rad
c_3	20N· m · s/rad	$c_4{'}$	10N· m · s/rad
c_4	60N· m · s/rad	ρ	190000N· m
k	94000N/rad	f	0.07m
u_n	0.07	G_z	7000N

In this section, the self-excited shimmy and force-excited shimmy are both simulated. To investigate the dynamic response of the shimmy system, L2 functions are selected as the disturbances. The initial state values of this system are set as $[\theta_1, \dot{\theta}_1, \theta_2, \dot{\theta}_2, \theta_3, \dot{\theta}_3, \theta_4, \dot{\theta}_4] = [0.02, 0, 0, 0, 0, 0, 0, 0]$. As shown in Fig.1, we assume that the structure of the front wheel shimmy model is symmetrical. Therefore, the shimmy

angles θ_1 and θ_2 almost are the same. We will just give the simulation analysis of θ_1.

The response of θ_1 under self-excited shimmy is shown in Fig.2 and Fig.3. As shown in phase diagram Fig.2, the shimmy phenomenon is shown as a closed stable limit cycle. θ_1 vibrates with a constant amplitude as shown in the time-domain diagram Fig.3. According to the analysis, the self-excited shimmy generates when the DEV-EW runs at a low velocity within 20-40 km/h.
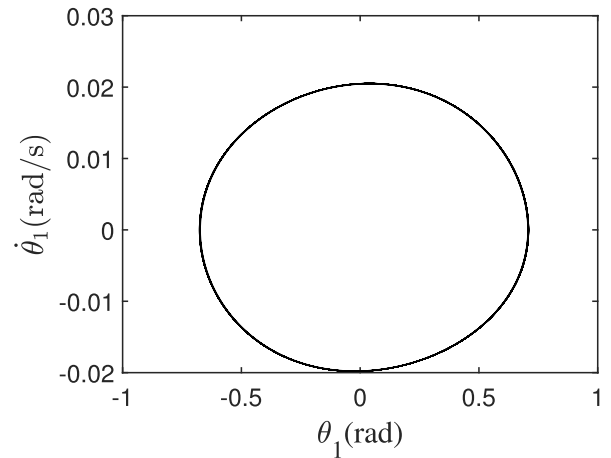

FIGURE 2. The phase diagram of shimmy angle θ_1 for self-excited shimmy.
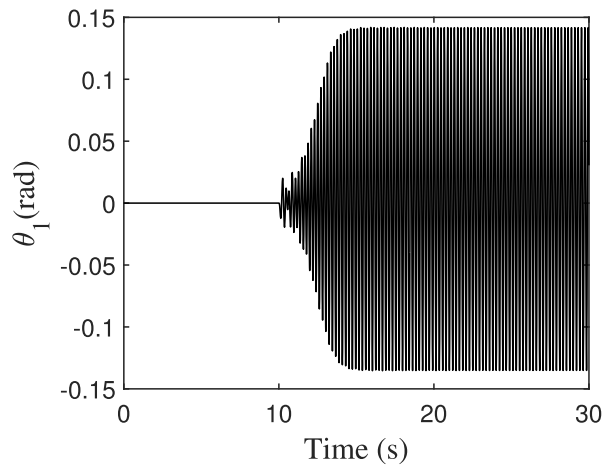

FIGURE 3. The time-domain diagram of shimmy angle θ_1 for self-excited shimmy.

In the force-excited shimmy simulation, the DEV-EW runs under 100 km/h and suffers the disturbance from 10th to 30th seconds. Fig.4 is the phase diagram of the θ_1 for force-excited shimmy suffering $100\sin(20t)/(1 + t^2)$N· m disturbance. It shows that the stable limit cycle vanishes gradually. θ_1 attenuates to zero as shown in time-domination diagram Fig.5.

As aforementioned analysis, the self-excited and force-excited shimmy simulation results are identical to other researchers' achievements, i.e., the built 4-DOF shimmy model is effective.
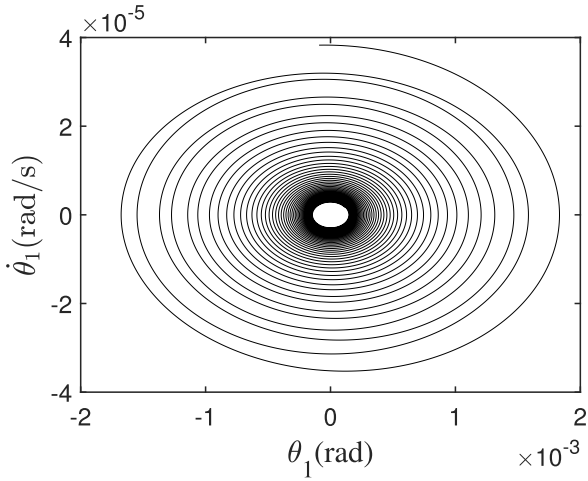
FIGURE 4. The phase diagram of shimmy angle θ_1 for force-excited shimmy.

B. THE SOFC METHOD SIMULATION

Now we will simulate the proposed SOFC method. In the simulation, we choose $L = 3$ and select $h^*(t) = 0.5$ as the sensor measurement error. The parameters of the designed controller and observer are listed in Tab.2.

TABLE 2. The parameters of the designed controller and observer.

Parameter	Nominal Value	Parameter	Nominal Value
$k1$	16000000	a_2	1.2
k_2	500000	a_3	1.5
k_3	5000	a_4	200
k_4	1120	a_5	20
k_5	179	a_6	600
k_6	18	a_7	12
k_7	1.1	a_8	3
k_8	0.025		

In order to verify the effectiveness of the SOFC method, the SMC method for the shimmy model is also designed and simulated. As definition in Eq.7, x_7 represents θ_1 in fact. Fig.6, Fig.7 and Fig.8 show that the estimation values of θ_1 can meet the requirement of the control system under different disturbances when the sensor measurement error is 0.5. Fig.9, Fig.10 and Fig.11 are the controller outputs for $100\sin(20t)/(1 + t^2)$N · m, $50\sin(20t)/(1 + t^2)$N · m and step disturbance respectively. Fig.12, Fig.13 and Fig.14 show the response of θ_1 under the SOFC, SMC and without control suffering $50\sin(20t)/(1 + t^2)$N · m, $100\sin(20t)/(1 + t^2)$N · m and step disturbance respectively. The simulation results under disturbance $50\sin(20t)/(1 + t^2)$N · m are shown in Tab.3. From which one obtains that θ_1 tends to zero after about 10s without control. The designed SOFC controller stabilizes θ_1 to zero within 2s. And the max value of θ_1 is attenuated within 0.008 rad. However, the SMC controller stabilizes θ_1 to zero within 4s. And the max value of θ_1 is attenuated within 0.015rad. The simulation results under disturbance $100\sin(20t)/(1 + t^2)$N · m are shown in Tab.4 which are similar with Tab.3. Tab.5 shows that the two

controller both do not shorten the stabilization time, θ_1 under SOFC controller has smaller oscillation value and is closer to the real added θ_1 than that under SMC controller. From the above figures and tables, one can find that the two controllers both have good anti-disturbance and can attenuate the shimmy phenomenon. But the proposed SOFC method has better effectiveness than the SMC method.

Remark 2: From Eq. 7 one can find that x_7 represents θ_1. $\hat{\theta}_1$ is obtained via observer Eq.12 in which a domination gain $L \geq 1$ is introduced to dominate the unknown nonlinear items and unknown sensor measurement error. If $L > 1$, the domination effect is obvious, but the estimation error becomes larger. Therefore, Fig.6 and Fig.7 show that the estimation values θ_1 do not coincide with the real values of θ_1 completely. But the estimation can meet the requirement.
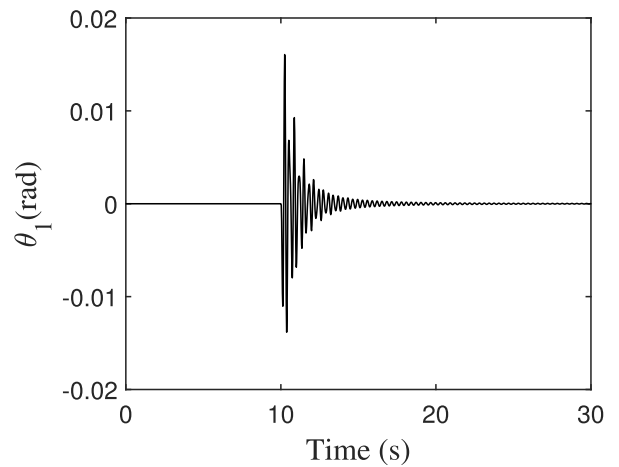

FIGURE 5. The time-domain diagram of shimmy angle θ_1 under force-excited shimmy.
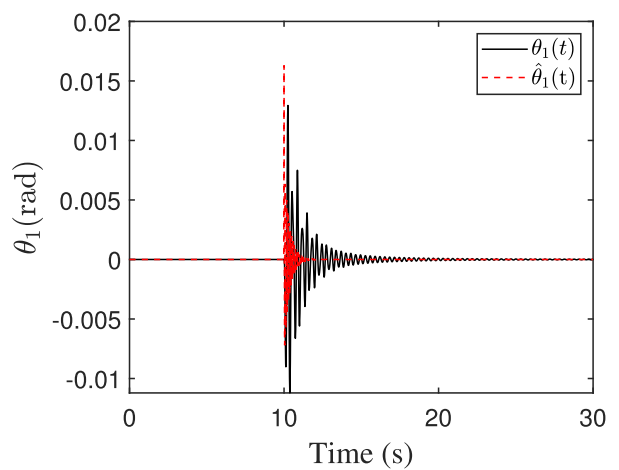

FIGURE 6. θ_1 and its estimation values under $v = 100$km/h suffering $100\sin(20t)/(1 + t^2)$ N · m.

According to the Hopf bifurcation theory, the self-excited shimmy is unstable, i.e, the self-excited shimmy can not be stabilized. Fig.15 shows the response of θ_1 with different controllers under self-excited shimmy. From which one can

**TABLE 3.** Simulation results under different controllers suffering $50\sin(20t)/(1+t^2)\,\text{N}\cdot\text{m}$.

Parameter	Without control	SMC	SOFC
max θ_1,rad	0.039	0.015	0.008
stability time of θ_1,s	10	4	2

TABLE 4. Simulation results under different controllers suffering $100\sin(20t)/(1+t^2)\,\text{N}\cdot\text{m}$.
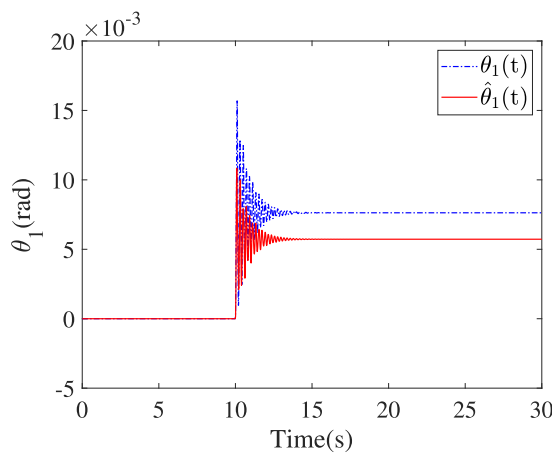
Parameter	Without control	SMC	SOFC
max θ_1,rad	0.078	0.024	0.014
stability time of θ_1,s	10	4	2

TABLE 5. Simulation results under different controllers suffering step disturbance.

| Parameter	Without control	SMC	SOFC
max θ_1,rad	0.013	0.017	0.008
stability time of θ_1,s	12	12	12
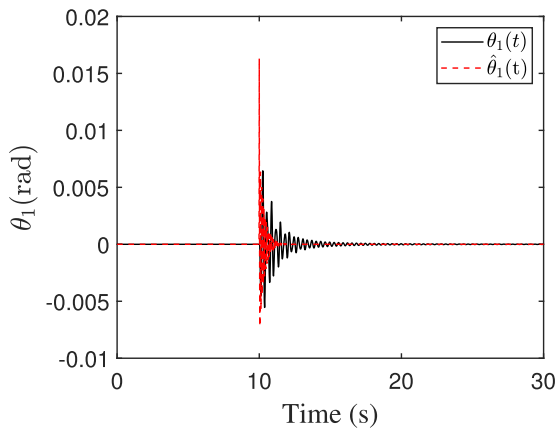
FIGURE 7. θ_1 and its estimation values under $v = 100$km/h suffering $50\sin(20t)/(1+t^2)\,\text{N}\cdot\text{m}$.


**FIGURE 8.** θ_1 and its estimation values under $v = 100$km/h suffering step disturbance.

find that the SOFC controller and SMC controller both can not enable θ_1 to converge to zero, but the SOFC controller also has better effectiveness than the SMC controller. The simulation result coincides with the Hopf bifurcation analysis. The simulation results are shown in Tab.6.
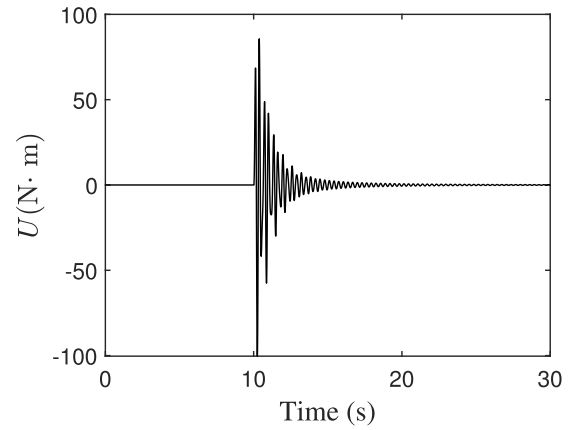
FIGURE 9. Controller output suffering $100\sin(20t)/(1+t^2)\,\text{N}\cdot\text{m}$.
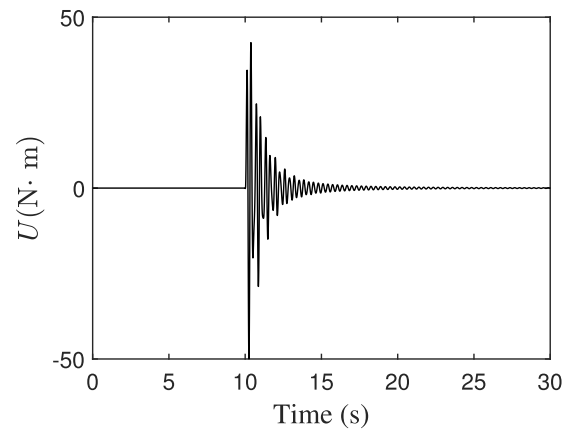
FIGURE 10. Controller output suffering $50\sin(20t)/(1+t^2)\,\text{N}\cdot\text{m}$.
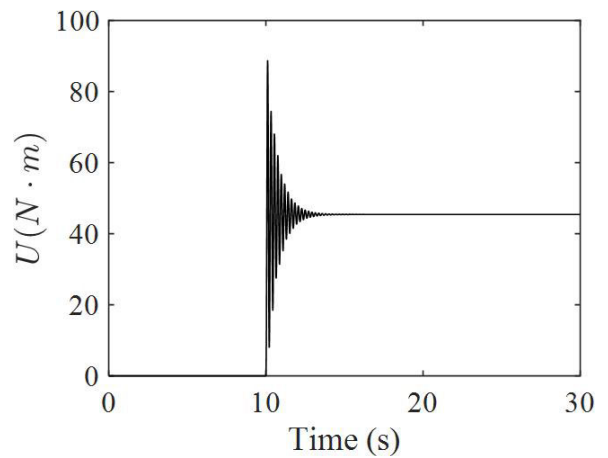
FIGURE 11. Controller output suffering step disturbance.

TABLE 6. Simulation results with different controllers for self-excited shimmy.

Parameter	Without control	SMC	SOFC
max θ_1,rad	0.142	0.115	0.068
stability time of θ_1,s	6	3	2

Remark 3: Generally speaking, we suggest to choose a smaller L under the premise of satisfying obvious
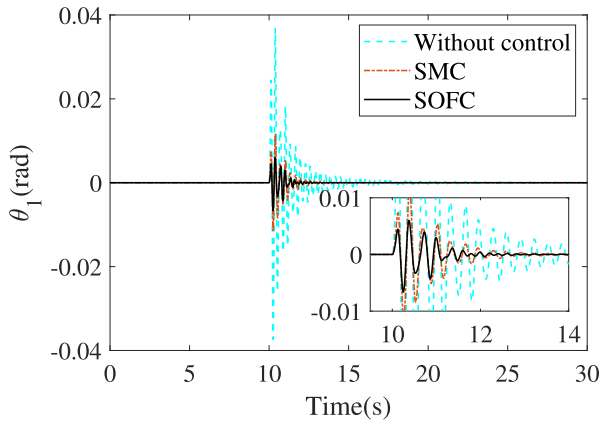
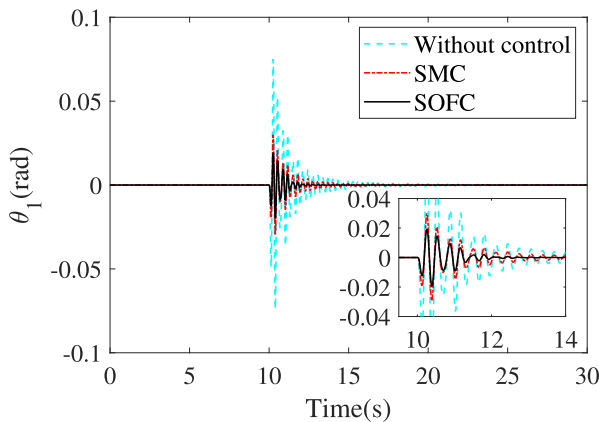**FIGURE 12.** Response of θ_1 under the SOFC, SMC and without control suffering $50\sin(20t)/(1+t^2)$ N · m.

FIGURE 13. Response of θ_1 under the SOFC, SMC and without control suffering $100\sin(20t)/(1+t^2)$ N · m.
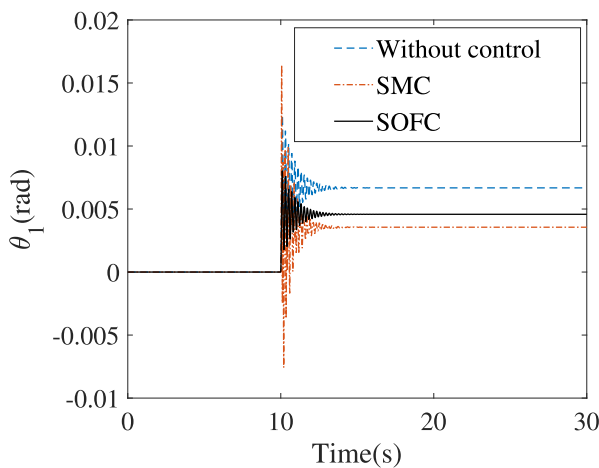

FIGURE 14. Response of θ_1 under the SOFC, SMC and without control suffering step disturbance.

anti-disturbance effect according to Eq.49. The allowable sensor measurement error h^* of the proposed method is determined by Eq.44. For verifying the anti-disturbance effect of the proposed method, we select a larger h^* according to Eq.44. But in fact, the sensor measurement error is not so large in practice.
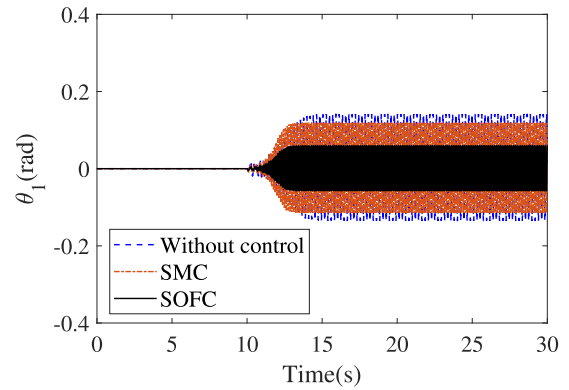

FIGURE 15. Response of θ_1 under the SOFC, SMC and without control under self-excited shimmy.

V. CONCLUSION

In this paper, for addressing the shimmy control issue for the DEV-EW considering the sensor measurement error and nonlinearities, the 4-DOF shimmy model of the front electric wheel is established and the dynamic functions of this model are obtained via Lagrange's theorem. Then the state equations of the shimmy control system with an unknown sensor measurement error and nonlinearities are presented. The SOFC method is proposed based on these state equations. This method consists of designing a linear sampled-data state observer which includes a domination gain as well as an output feedback control law for the shimmy control system. The domination gain can suppress the negative influence caused by the unknown sensor measurement error and nonlinearities. By the Lyapunov method, the proposed SOFC method is proved that it can stabilize the shimmy system globally asymptotically. Finally, simulations are carried out to verify the effectiveness of the constructed 4-DOF shimmy model. And the proposed SOFC method is also verified compared with the SMC method. The simulation results show that the SOFC method has a better effect than the traditional SMC method for active shimmy control,i.e., the designed SOFC method can address the sensor measurement error issue effectively.

CONFLICT OF INTEREST

The authors declare that they have no conflict of interest.

REFERENCES

[1] M. Blau, G. Akar, and J. Nasar, "Driverless vehicles' potential influence on bicyclist facility preferences," *Int. J. Sustain. Transp.*, vol. 12, no. 9, pp. 665–674, Oct. 2018.

[2] K. Kaur and G. Rampersad, "Trust in driverless cars: Investigating key factors influencing the adoption of driverless cars," *J. Eng. Technol. Manage.*, vol. 48, pp. 87–96, Apr. 2018.

[3] R. Kottasz, R. Bennett, R. Vijaygopal, and B. Gardasz, "Driverless futures: Current non-drivers' willingness to travel in driverless vehicles," *J. Marketing Manage.*, vol. 37, nos. 15–16, pp. 1–34, 2021.

[4] A. K. Kiss, S. S. Avedisov, D. Bachrathy, and G. Orosz, "On the global dynamics of connected vehicle systems," *Nonlinear Dyn.*, vol. 96, no. 3, pp. 1865–1877, May 2019.

[5] T. Mi, G. Stepan, D. Takacs, N. Chen, and N. Zhang, "Model establishment and parameter analysis on shimmy of electric vehicle with independent suspensions," *Proc. IUTAM*, vol. 22, pp. 259–266, Jan. 2017.

[6] T. Mi, G. Stepan, D. Takacs, and N. Chen, "Shimmy model for electric vehicle with independent suspensions," *Proc. Inst. Mech. Eng. D, J. Automobile Eng.*, vol. 232, no. 3, pp. 330–340, Feb. 2018.

[7] S. Beregi, D. Takacs, and G. Stepan, "Bifurcation analysis of wheel shimmy with non-smooth effects and time delay in the tyre–ground contact," *Nonlinear Dyn.*, vol. 98, no. 1, pp. 841–858, Oct. 2019.

[8] H. B. Pacejka, "Analysis of the shimmy phenomenon," *Proc. Inst. Mech. Eng., Automobile Division*, vol. 180, no. 1, pp. 251–268, Jan. 1965.

[9] J.-W. Lu, J. Gu, and M.-J. Liu, "Modeling of the vehicle shimmy system with consideration of clearance of the steering linkage mechanism," *Meccanica*, vol. 45, no. 1, pp. 53–61, Feb. 2010.

[10] H. Wei, J. Lu, and J. Jiang, "Analysis of dynamic behavior of vehicle shimmy system with stochastic clearance," *Mech. Solids*, vol. 57, no. 1, pp. 139–148, Feb. 2022.

[11] V. P. Zhuravlev, D. M. Klimov, and P. K. Plotnikov, "A new model of shimmy," *Mech. Solids*, vol. 48, no. 5, pp. 490–499, Sep. 2013.

[12] S. Ran, I. J. M. Besselink, and H. Nijmeijer, "Energy analysis of the Von Schlippe tyre model with application to shimmy," *Vehicle Syst. Dyn.*, vol. 53, no. 12, pp. 1795–1810, Dec. 2015.

[13] C. Bian, N. Zhang, G. Li, G. Yin, and N. Chen, "Suspension damping characteristics influence on the wheel shimmy of 4 WID electric vehicles," in *The Dynamics of Vehicles on Roads and Tracks*. Boca Raton, FL, USA: CRC Press, 2017, pp. 413–418.

[14] W. Daogao, J. Tong, C. Changhe, J. Yibin, P. Ning, and P. Zhijie, "Hopf bifurcation character of an interactive vehicle–road shimmy system under bisectional road conditions," *Proc. Inst. Mech. Eng. D, J. Automobile Eng.*, vol. 231, no. 3, pp. 405–417, Feb. 2017.

[15] D. Wei, W. Zhai, Y. Zhu, G. Jiang, A. Yin, and B. Zhang, "Self-excited vibration of whole vehicle with multiple limit cycles induced by shimmy of front wheels," *J. Low Freq. Noise, Vibrat. Act. Control*, vol. 39, no. 4, pp. 1052–1064, Dec. 2020.

[16] L. Cheng, H. Cao, and L. Zhang, "Two-parameter bifurcation analysis of an aircraft nose landing gear model," *Nonlinear Dyn.*, vol. 103, no. 1, pp. 367–381, Jan. 2021.

[17] S. Beregi, "Nonlinear analysis of the delayed tyre model with control-based continuation," *Nonlinear Dyn.*, vol. 110, no. 4, pp. 3151–3165, Dec. 2022.

[18] S. Dutta and S.-B. Choi, "Control of a shimmy vibration in vehicle steering system using a magneto-rheological damper," *J. Vibrat. Control*, vol. 24, no. 4, pp. 797–807, Feb. 2018.

[19] Q. Meng, C. Qian, and Y. Shu, "Active steering wheel shimmy control for electric vehicle by sampled-data output feedback," *ISA Trans.*, vol. 84, pp. 262–270, Jan. 2019.

[20] Q. Meng, C. Qian, C. Hu, Z. Sun, and P. Wang, "Finite-time active shimmy control based on uncertain disturbance observer for electric vehicle with independent suspension," *IET Intell. Transp. Syst.*, vol. 14, no. 13, pp. 1835–1844, Dec. 2020.

[21] Z.-Y. Sun, K. Zhang, C.-C. Chen, and Q. Meng, "Robust output feedback control of time-delay nonlinear systems with dead-zone input and application to chemical reactor system," *Nonlinear Dyn.*, vol. 109, no. 3, pp. 1617–1627, Aug. 2022.

[22] J. Zhang and G. Yang, "Global finite-time output stabilization of nonlinear systems with unknown measurement sensitivity," *Int. J. Robust Nonlinear Control*, vol. 28, no. 16, pp. 5158–5172, Nov. 2018.

[23] S.-Y. Oh and H.-L. Choi, "A further result on global stabilization of a class of nonlinear systems by output feedback with unknown measurement sensitivity," *Int. J. Control, Autom. Syst.*, vol. 17, no. 10, pp. 2500–2507, Oct. 2019.

[24] S.-Y. Oh and H.-L. Choi, "Regulation of a class of nonlinear systems with unknown growth rate under uncertain measurement sensitivity," *J. Electr. Eng. Technol.*, vol. 16, no. 5, pp. 2767–2775, Sep. 2021.

[25] M.-S. Koo and H.-L. Choi, "Output feedback regulation of a class of lower triangular nonlinear systems with arbitrary unknown measurement sensitivity," *Int. J. Control, Autom. Syst.*, vol. 18, no. 9, pp. 2186–2194, Sep. 2020.

[26] C.-Y. Liu, Z.-Y. Sun, Q. Meng, and W. Sun, "Robust control of high-order nonlinear systems with unknown measurement sensitivity," *Sci. China Inf. Sci.*, vol. 64, no. 6, pp. 1–3, Jun. 2021.

[27] C. Qian, S. He, and Y. Zou, "Compensator-based output feedback stabilizers for a class of planar systems with unknown structures and measurements," *IEEE Trans. Autom. Control*, vol. 67, no. 4, pp. 2138–2143, Apr. 2022.

[28] Y. Deng, Z. Liu, and B. Chen, "Event-triggered adaptive neural tracking control of nonstrict-feedback nonlinear systems with unknown measurement," *Nonlinear Dyn.*, vol. 109, no. 2, pp. 863–875, Jul. 2022.

[29] C. Qian and W. Lin, "A continuous feedback approach to global strong stabilization of nonlinear systems," *IEEE Trans. Autom. Control*, vol. 46, no. 7, pp. 1061–1079, Jul. 2001.

[30] P. Wang, L. Chai, C. Chen, and S. Fei, "Global sampled-data output-feedback stabilization for nonlinear systems with unknown measurement sensitivity," *Int. J. Robust Nonlinear Control*, vol. 29, no. 14, pp. 4909–4927, Sep. 2019.

QINGHUA MENG received the Ph.D. degree from Zhejiang University, China, in 2005. Since 2005, he has been with the School of Mechanical Engineering, Hangzhou Dianzi University, where he is currently a Professor. His current research interests include electric vehicle stability control and mechanical fault diagnosis and signal processing.

SHENCHENG ZHAO is currently pursuing the Graduate degree with the School of Mechanical Engineering, Hangzhou Dianzi University. His current research interests include electric vehicle stability control and electric vehicle shimmy control.
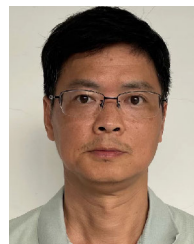
RONG LIU received the Ph.D. degree from Zhejiang University, China, in 2004. Since 2006, he has been with the School of Mechanical Engineering, Hangzhou Dianzi University, where he is currently an Associate Professor. His current research interests include mechanical design and mechatronic control.

ZONG-YAO SUN received the Ph.D. degree in control engineering from Shandong University, China, in 2009. He has been a Professor in control theory with the Institute of Automation, Qufu Normal University, Qufu, China. His current research interests include robust and adaptive control and nonlinear system theory.

HAIBIN HE received the Ph.D. degree from Zhejiang University, China, in 2017. He is currently with Ningbo C.S.I. Power & Machinery Group Company Ltd., where he is also an Associate Research Fellow. His current interests include control system design, mechanical fault diagnosis, and signal processing.

• • •